Tree Physiology 38, 1166–1179
doi:10.1093/treephys/tpy032

Research paper

Gas exchange by the mesic-origin, arid land plantation species *Robinia pseudoacacia* under annual summer reduction in plant hydraulic conductance

Yoshiyuki Miyazawa[1,2,7], Sheng Du[3], Takeshi Taniguchi[4], Norikazu Yamanaka[4] and Tomo'omi Kumagai[5,6]

[1]Department of Geography, University of Hawai'i at Manoa, Honolulu, HI 96822, USA; [2]Research Institute for East Asian Environments, Kyushu University, 744 Motooka, Fukuoka 819-0395, Japan; [3]State Key Laboratory of Soil Erosion and Dryland Farming on Loess Plateau, Institute of Soil and Water Conservation, Chinese Academy of Sciences and Ministry of Water Resources, Yangling, Shaanxi 712100, China; [4]Aridland Research Center, Tottori University, Hamasaka, Tottori, Japan; [5]Institute for Space-Earth Environmental Research, Nagoya University, Nagoya 464-8601, Japan; [6]Graduate School of Agricultural and Life Sciences, The University of Tokyo, 1-1-1 Yayoi, Bunkyo-ku, Tokyo 113-8657, Japan; [7]Corresponding author (sclerophyll@gmail.com)

Received August 9, 2017; accepted March 6, 2018; published online March 28, 2018; handling Editor Nathan Phillips

The mesic-origin plantation species *Robinia pseudoacacia* L. has been successfully grown in many arid land plantations around the world but often exhibits dieback and reduced growth due to drought. Therefore, to explore the behavior of this species under changing environmental conditions, we examined the relationship between ecophysiological traits, gas exchange and plant hydraulics over a 3-year period in trees that experienced reduced plant hydraulic conductance (G_p) in summer. We found that the transpiration rate, stomatal conductance (G_s) and minimum leaf water potential (Ψ_{lmin}) decreased in early summer in response to a decrease in G_p, and that G_p did not recover until the expansion of new leaves in spring. However, we did not observe any changes in the leaf area index or other ecophysiological traits at the leaf level in response to this reduction in G_p. Furthermore, model simulations based on measured data revealed that the canopy-scale photosynthetic rate (A_c) was 15–25% higher than the simulated A_c when it was assumed that Ψ_{lmin} remained constant after spring but almost the same as the simulated A_c when it was assumed that G_p remained high even after spring. These findings indicate that *R. pseudoacacia* was frequently exposed to a reduced G_p at the study site but offset its effects on A_c by plastically lowering Ψ_{lmin} to avoid experiencing any further reduction in G_p or G_s.

Keywords: leaf ecophysiological traits, photosynthesis, plant hydraulic, *Robinia pseudoacacia*, stomatal conductance.

Introduction

Plants need to photosynthesize to obtain sufficient carbon for growth and survival (Farquhar and Sharkey 1982). However, the uptake of CO_2 for photosynthesis requires the opening of stomata, which promotes transpiration (E) and thus reduces the leaf water potential (Ψ_l). When plants experience excessive transpiration and a large associated reduction in Ψ_l, they reduce the hydraulic conductance of liquid water from the roots to the leaves (G_p) (Meinzer et al. 1999) and the stomatal conductance (G_s) (Hubbard et al. 2001). Thus, plants are able to control G_s under changing atmospheric and soil water conditions to avoid an excessive reduction in Ψ_l (Tyree and Sperry 1988, Jones and Sutherland 1991, Oren et al. 1999), allowing them to maintain Ψ_l near the critical level to prevent cavitation (Choat et al. 2012).

Stomatal control for the maintenance of Ψ_l often involves dynamic changes in ecophysiological traits at the leaf scale (Bucci et al. 2006, Miyazawa et al. 2014, Binks et al. 2016). While many species respond to increasing evaporative demands by reducing G_s and the net photosynthetic rate (A) to maintain Ψ_l and G_p at safe levels, i.e., isohydric behavior (Oren et al.

1999, Meinzer et al. 2009), some species maintain G_s and A at high levels while experiencing further reductions in Ψ_l and G_p, i.e., anisohydric behavior (Manzoni et al. 2013), which increases the risk of a further reduction in each of these parameters (Hubbard et al. 2001, Domec et al. 2009). Since such species-specific responses to changing soil moisture and evaporative demands determine the gas exchange rates (A and E) of forests, knowledge of these is important, particularly in temperate regions where half of the plant growing season occurs during and after the hot summer with high vapor pressure deficit (D).

The plantation species *Robinia pseudoacacia* L. has been intensively planted in semiarid regions around the world. This species originated from a mesic region in North America but grows well in dry environments, as evidenced by the fact that it has successfully covered a large amount of previously bare lands in the Loess Plateau in China through the establishment of intensive plantations (Zheng and Wang 2014). However, dieback is often observed in these trees both in the Loess Plateau and in coastal sandy areas in Japan (Yamanaka et al. 2014), indicating that they frequently experience reductions in G_p (cf. Adams et al. 2009). Therefore, *R. pseudoacacia* is thought to have species-specific ecophysiological strategies both for avoiding excessive E under increasing evaporative demands and decreasing soil moisture levels (Tanaka-Oda et al. 2010, Du et al. 2011, Chen et al. 2014), and for enhancing carbon gains even under a reduced G_p, such as by maintaining a high G_s while experiencing further reductions in Ψ_l (Kumagai and Porporato 2012). However, although there is a large body of evidence around the use of stomatal control to avoid a reduction in G_p (Jones and Sutherland 1991, Oren et al. 1999) and the time course of reduced G_p in plants (Hacke et al. 2000, Wang et al. 2014), few studies have investigated gas exchange and related plant hydraulics in plants that experience dynamic changes in G_p (Saliendra et al. 1995, Anderegg et al. 2014), and even fewer have focused on the mitigation of the impacts on carbon gain.

Therefore, in this study, we examined how *R. pseudoacacia* improves its carbon gain and/or alleviates the environmental impact of seasonal drought conditions by investigating the leaf- and tree-level ecophysiological traits of trees growing in a monospecific stand in a temperate forest. We first monitored E over a 3-year period to obtain sap flux measurements, which we used to reveal the time course of plant hydraulics. We then used the obtained parameters to independently compute canopy-scale A and E (A_c and E_c, respectively), and also simulated A_c under different levels of the ecophysiological trait parameters to predict alternative potential responses to a changing environment by *R. pseudoacacia* and thus the contribution of each ecophysiological trait toward gas exchange and plant hydraulics (Williams et al. 1998). In particular, we addressed three main questions: (i) Is there clear seasonality in ecophysiological traits across years under different environmental conditions? (ii) Do the trees maintain a daily minimum Ψ_l (Ψ_{lmin}) at a relatively high and constant level or allow Ψ_l to drop to very low values under evaporative conditions? (iii) How is the observed behavior advantageous over other possible strategies in this environment?

Materials and methods

Study site and meteorological conditions

This study was conducted in a 20 m × 20 m plot for sap flux monitoring that was located in a 3-ha monospecific *R. pseudoacacia* plantation situated on a sand dune at the Arid Land Research Center, Tottori University, Tottori, Japan (35°32′13″N, 134°12′34″E, 20 m above sea level) from summer 2011 until spring 2015. This region has a cool temperate climate with snow cover in winter (end of November to early–mid-March).

A weather station on top of a nearby building (25-m high) monitored the climatic conditions with a pyranometer (P-MS-402; Ogasawara-Keiki Co., Ltd, Tokyo, Japan), a rainfall gage (TK-1; Takeda Keiki Co., Ltd, Tokyo, Japan), air temperature–humidity sensors (JS-252 N; Ogasawara-Keiki Co., Ltd) and an anemometer (WS-B56; Ogasawara-Keiki Co., Ltd), the data from which were recorded at 1-h intervals by a data logger (OKSAM-4100; Ogasawara-Keiki Co., Ltd). A second weather station located in a nearby open place monitored the climatic conditions with a photosynthetically active radiation (PAR) sensor (S-LIA-M003; Onset Computer Corporation, Bourne, MA, USA), an anemometer (S-WSA-M003; Onset Computer Corporation) and air temperature–humidity sensors (S-THB-M002; Onset Computer Corporation), the data from which were recorded at 10-min intervals by a data logger (U12-008; Onset Computer Corporation). The outputs from this second weather station were calibrated against those obtained by the first weather station and were used for subsequent analyses.

The annual average air temperature at the study site was 15.1 °C between 2005 and 2014, with a maximum mean monthly temperature of ~30 °C in July–August during 2012–14 (Figure 1). The mean annual precipitation for the period 2005–14 was 1939 mm, with a rainy season generally occurring from late May to late July but rainy days continuing into August in 2014. Soil moisture in the sap flux monitoring plot was measured as the volumetric soil water content using EC-5 sensors (Decagon Devices, Pullman, WA, USA) installed at soil depths of 10, 30, 70 and 100 cm (one sensor at each depth). The data were scanned every 1 min and the daily means of soil moisture were recorded by a data logger (CR1000; Campbell Scientific, Logan, UT, USA) each day. While soil moisture fluctuated from 0.01 to 0.05 $m^3 m^{-3}$ at a depth of 10 cm, it ranged from 0.04 to 0.05 $m^3 m^{-3}$ below 30 cm, suggesting that there was no obvious drought at this site during the study period. The soil at the study site was composed of sand, the hydraulic properties of which have been previously discussed by Kondo and Xu (1997).

Understory herbs appear in the plantation in spring and then disappear after the end of the rainy season in July due to a

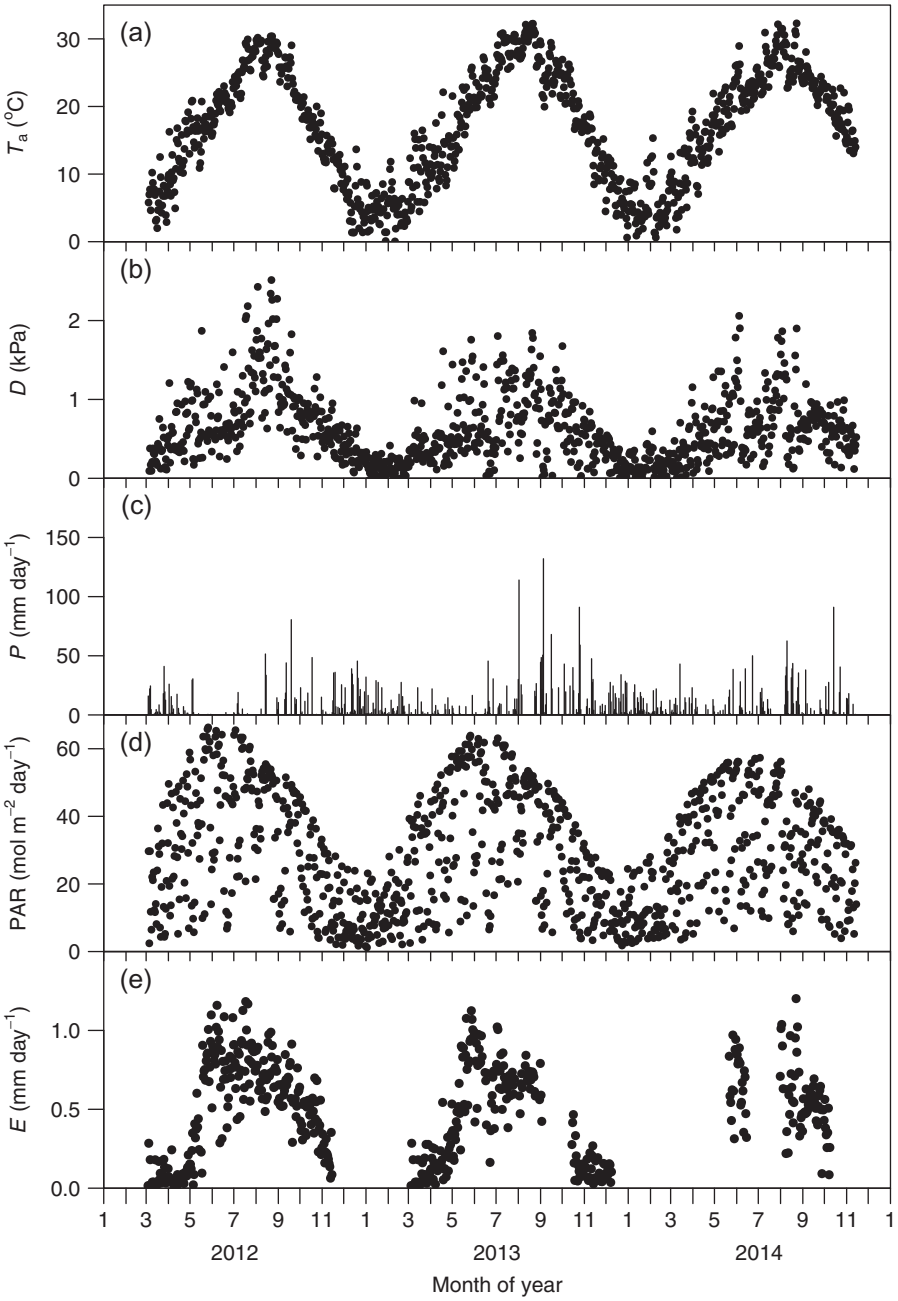

Figure 1. Seasonal trends in (a) air temperature (T_a), (b) vapor pressure deficit (D), (c) precipitation (P), (d) photosynthetically active radiation (PAR) and (e) transpiration rate (E) at the study site from 2012 to 2014.

reduction in surface soil moisture. Details of the stand characteristics are shown in Table 1. We measured the mean diameter at breast height (DBH, cm) of each of 12 sample trees that were used for sap flux monitoring (see below) at a height of 1.3 m above the ground every year after summer 2011. We also measured the height of all of the trees in the monitoring plot in October 2014. To measure the leaf area index (LAI, $m^2\ m^{-2}$), we periodically took hemispherical photographs at eight fixed points in the plot using a digital camera (Nikon CoolPix 990; Nikon Corporation, Tokyo, Japan) with a fisheye lens (fisheye converter, FC-E 8; Nikon Corporation) and then analyzed these using image analysis software (HemiView Canopy Analysis Software Version 2.1; Delta-T Devices, Cambridge, UK).

In 2015, we determined the root distribution and fine root length of trees by digging four 1.5-m-deep holes (Table 1). We collected fine roots (<2 mm diameter) by taking cylindrical soil cores (100 ml) at various depths (10, 30, 50, 70 and 100 cm) and hand sorting the samples. Images of the fine roots were then scanned onto a computer and the root length per unit soil volume was determined using the image analysis software Scion Image for Windows Alpha 4.0.3.2 (Scion Corporation, Frederick, MD, USA) and RootLength 1.80 win (Kimura and Yamasaki

2003). We did not find any fine roots at a depth >70 cm, indicating that the soil moisture level of the entire rooting zone was covered by the soil moisture sensors.

Sap flow measurements

We monitored the xylem sap flux density (F_d, g m^{-2} s^{-1}) by installing Granier-type sap flux sensors (Granier 1987) with a modified length (James et al. 2002) on 12 sample trees in August 2011 (Table 2). Each sensor consisted of two 10-mm-long probes (a heated probe and reference probe) that were inserted into the stem at breast height. To avoid solar radiation affecting the temperature data, each sensor was shielded by an aluminum cover and a heat insulator. We selected trees with different DBHs that reflected the overall DBH distribution in the plot. For the non-destructive estimation of sapwood area, we collected incremental cores from two sides of the stem at breast height on each sample tree in October 2014. The color of the sapwood was visibly different from the heartwood. Therefore, based on the assumption that the cross section of the stem and the heartwood was round, we calculated the sapwood area (S_{sap}, m^2) of each tree during the monitoring period (2011–14) according to the DBH in each year and the bark thickness. Because the sapwood area was narrow, we assumed that each sensor covered the entire range along the radial profile of the sapwood. The established relationship between the cross-section area and S_{sap} was then used to calculate S_{sap} in each year.

To monitor the circumferential variation in sap flux, we installed one sensor in a random azimuthal direction and another sensor on the opposite side of the stem in each sample tree. Since the sapwood was wider than the sensor length in all of the sample trees, we assumed that all of the sensors were installed inside the sapwood and so did not apply the correction proposed by Clearwater et al. (1999). We periodically checked the sensors for breakage and replaced them where this had occurred (every 6–12 months). Most of the sensors were replaced within 1 year and so the effect of long-term installation on the sapwood and sap flux was considered negligible. A data logger (CR1000; Campbell Scientific) with an attached multiplexer (AM16/32; Campbell Scientific) scanned the difference in temperature between the heated probe and reference probe (ΔT, °C) at 10-s intervals and recorded the average value at 10-min intervals.

ΔT was converted to F_d using the equation proposed by Granier (1987). This required the determination of ΔT_{max}, which represents ΔT at $F_d = 0$. At our study site, D (kPa) did not reach zero even at predawn from late spring until early autumn, implying the existence of nighttime transpiration. Furthermore, even in the absence of nighttime transpiration, refilling of the stored water inside the plant body can lead to positive F_d values throughout the night. Therefore, to avoid underestimating ΔT_{max} and F_d due to positive F_d values at nighttime, we calculated ΔT_{max} based on the method proposed by Oishi et al. (2008), which assumes that ΔT_{max} is achieved on nights when (i) D is <0.05 kPa for two consecutive hours and (ii) during this 2-h period, the coefficient of variation for ΔT is <0.5%. However, since there was a series of 20–25 days in August 2012 and 2013 where the minimum D was >0.05 kPa, we used 0.15 kPa rather than 0.05 kPa for the criterion in (i) when calculating ΔT_{max}. We found that there was little difference in F_d or the daily cumulative F_d in May–June 2012 and 2013 regardless of whether 0.15 kPa or 0.05 kPa was used as the threshold for filtering ΔT_{max} (data not shown). On days that did not meet the criteria of Oishi et al. (2008), we linearly interpolated the values for ΔT_{max} from the values on days that did meet the criteria.

The stand mean xylem sap flux over the total stand sapwood area (J_s, g m^{-2} s^{-1}) was calculated following Kumagai et al. (2007):

Table 1. Characteristics of the *Robinia pseudoacacia* stand at the study site.

Characteristic	Value
Standing tree density (ha^{-1})	2500
Mean DBH[1] (cm)	11.26 ± 5.59[2]
Basal area (m^2 ha^{-1})	22.89
Sapwood area (m^2 ha^{-1})	5.64
Root length (10^3 m m^{-2})	
Total	1.98
10 cm	0.81
30 cm	0.46
50 cm	0.50
70 cm	0.21

[1]DBH, diameter at breast height.
[2]Mean ± standard deviation.

Table 2. Characteristics of the 12 *Robinia pseudoacacia* sample trees used for sap flux monitoring.

Tree no.	DBH[1,2] (cm)	Height[3] (m)	Sapwood depth[2] (cm)
1	20.8	14.5	1.01
2	17.4	12.9	1.13
3	13.7	8.0	1.04
4	9.8	8.0	1.25
5	23.7	10.9	1.57
6	16.1	10.5	1.25
7	10.6	7.7	1.23
8	20.9	11.6	1.45
9	8.7	N.A.	1.36
10	18.8	10.5	1.22
11	12.9	8.32	1.37
12	14.8	7.7	1.24

[1]DBH, diameter at breast height.
[2]Data obtained at the start of monitoring (August 2011).
[3]Data obtained at the end of monitoring (November 2014).

$$J_s = \frac{\sum_{i=1}^{N} S_{sapi} \cdot F_{di}}{\sum_{n=1}^{N} S_{sapi}} \quad (1)$$

where subscript i denotes the sample tree number and N is the sample size, which changed over time due to the breakage of sensors. E (g m^{-2} s^{-1}) was calculated at the stand level using total S_{sap} (S_{sap_total}, m^2), the ground area of the plot (S_G, m^2), and J_s as follows:

$$E = J_s \frac{S_{sap\_total}}{S_G} \quad (2)$$

Daily E (E_{day}, mm day^{-1}) was also calculated using S_{sap_total}/S_G and daily J_s (J_{s_day}, mm day^{-1}).

Given the small size of *R. pseudoacacia* leaflets and the consistent winds at the study site, we assumed that the leaf surface was well coupled to the atmosphere. Therefore, we approximated G_s (mol m^{-2} s^{-1}) using the following equation:

$$G_s = \frac{K_G c}{LAI} \cdot \frac{E}{D} \times 10^{-3} \quad (3)$$

where K_G is a conversion function that is calculated as $115.8 + 0.4226T_a$ (kPa m^3 kg^{-1}) (Phillips and Oren 1998), T_a is the air temperature, and c is the molar air density (mol m^{-3}). Although stem water storage may cause a time lag between the measured J_s at the stem and transpiration at the leaf surface (i.e., E may not be equal to $J_s \cdot S_{sap\_total}/S_G$ at a particular point in time), like Chen et al. (2014), we did not find a clear time lag between the diurnal variations in J_s and D, possibly due to the modest contribution of plant storage water to E in *R. pseudoacacia* (Jupa et al. 2016). Therefore, we used E from Eq. (2) in Eq. (3).

We determined the relationship between G_s and D by performing a boundary line analysis under high solar radiation (>600 W m^{-2}) (Naithani et al. 2012) by (i) partitioning the data for the G_s response to D into bins (0.3-kPa intervals); (ii) calculating the mean and standard deviation (SD) of light-saturated G_s within each D bin; (iii) removing outliers ($P = 0.05$, Dixon's test; Sokal and Rohlf 1995); and (iv) selecting values of G_s that were greater than the mean plus 1 SD to obtain the boundary line data. In each month, we obtained the relationship between G_s and D using the following equation:

$$G_s = G_{sref} - \delta \ln(D) \quad (4)$$

where δ is the slope [mol m^{-2} s^{-1} $\ln(kPa)^{-1}$] and G_{sref} is the reference G_s (mol m^{-2} s^{-1}), which denotes the intercept at D = 1 kPa. The ratio of δ to G_{sref} was obtained for each month and compared with the theoretical value of 0.6 for isohydric leaves with perfect stomatal control of minimum Ψ_l (Oren et al. 1999).

Leaf ecophysiological trait measurements

Leaf-level ecophysiological traits were periodically measured between August 2012 and October 2014. We determined the relationship between the net photosynthetic rate (A, μmol m^{-2} s^{-1}) and the intercellular CO_2 concentration (C_i, μmol mol^{-1}) (A–C_i relationship) using a portable photosynthesis measurement system (Li-6400; Li-COR, Lincoln, NE, USA). Photosynthetic measurements were taken from trees growing near the sample trees that were selected for sap flux monitoring using intact, fully expanded leaves from well-exposed crown parts at the top of the canopy near a scaffolding tower (2012 and 2013) or within reach from the ground (2014). Three trees were selected and 8–11 leaves per tree were used to measure the A–C_i relationship.

We first measured leaf-scale A and the stomatal conductance for H_2O (g_{sw}, mol m^{-2} s^{-1}) at light saturation (PAR = 1500 μmol m^{-2} s^{-1}), ambient air temperature (20–31 °C) and a CO_2 concentration of 380 μmol mol^{-1} in a cuvette. Light was supplied by an attached light source (Li-6400-2B; Li-COR) and the vapor pressure deficit of the cuvette air was <1.5 kPa. Once the gas exchange rates had stabilized, the environmental conditions inside the cuvette were fixed. Measurements were completed in the early morning to allow C_i to be calculated precisely because g_{sw} and A dropped drastically in the afternoon in May and June or after 10:00 h in July–October. We then measured light-saturated A at six levels of CO_2 concentration to determine the maximum rate of ribulose-1,5-bisphosphate (RuBP) carboxylation by RuBP carboxylase/oxygenase (Rubisco) (V_{cmax}, μmol m^{-2} s^{-1}), as described by Farquhar et al. (1980). V_{cmax} was obtained by regressing A against C_i according to the equations provided in Farquhar et al. (1980) at CO_2 concentrations of <400 μmol mol^{-1} and using the values of the Rubisco Michaelis–Menten constants for CO_2 and O_2, and the CO_2 compensation point provided in von Caemmerer et al. (1994) and Harley et al. (1992). Photosynthetic capacity was calculated as V_{cmax} at a common leaf temperature of 25 °C (V_{cmax25}), according to the equation provided by Harley et al. (1992) and the parameters for temperature dependencies provided by de Pury and Farquhar (1997). Following these photosynthesis measurements, the leaves were kept in the dark for more than 20 min to measure the dark respiration rate (R_d, μmol m^{-2} s^{-1}) at a leaf temperature of 20–30 °C. The gas exchange rates of leaves in the shade at the bottom of the crown were also measured to characterize the vertical profile of V_{cmax25}.

During the same period as the A–C_i relationship was measured, the diurnal changes in leaf gas exchange rates were monitored at 1- to 3-min intervals in four leaves from each of three trees to determine the parameters in the stomatal sensitivity model. The environmental conditions inside the cuvette were the same as the ambient conditions, with ambient light being allowed to enter through the transparent cuvette top and the temperature being maintained using a Li-6400 temperature controller. The intrinsic level of stomatal conductance for CO_2 (g_{sc}) and its response to environmental factors was expressed using the slope (m) of the g_{sc} formula proposed by Ball et al. (1987):

$$g_{sc} = m\frac{Ah_r}{C_s} + b \quad (5)$$

where C_s is CO_2 concentration (μmol mol^{-1}) and h_r is relative humidity at leaf surface (Figure 1).

We assessed the leaf water status by measuring Ψ_l (MPa) using a Scholander-type pressure chamber (PMS Instruments Ltd, Corvallis, OR, USA) with N_2 balancing gas. In each measurement period, Ψ_l was measured in three sample trees for photosynthesis measurements using six leaves per tree located on the sun-exposed side of the crown surface. The leaf water potential was measured predawn (Ψ_{l_pre}, MPa), in the early morning (9:00–10:00 h), and at midday (Ψ_{l_mid}, MPa; 12:00–14:00 h) under sunny conditions. In May, July and October 2014, Ψ_l was also measured continuously from 9:00 until 16:00 h to determine diurnal variations in this parameter. Leaves on the same current-year shoot as those that were being used to measure Ψ_l were covered with aluminum foil and plastic bags containing wet filter paper at predawn to protect them from solar radiation and the associated transpiration. Based on the assumption that water flow between the leaves and the stem xylem was at equilibrium, Ψ_l of the covered leaves was treated as the stem water potential (Ψ_{stem}, MPa; three leaves per tree). We assumed that Ψ_{l_mid} represented Ψ_{lmin}, which was used in a later model simulation in which trees control stomata to prevent Ψ_l from becoming lower than Ψ_{lmin} (Williams et al. 1996).

G_p (g m^{-2} s^{-1} MPa^{-1}) was calculated using the midday J_s (J_{s_mid}, g m^{-2} s^{-1}) or E (E_{mid}, g m^{-2} s^{-1}) value as:

$$G_p = \frac{J_{s\_mid}}{\Psi_{l\_pre} - \Psi_{l\_mid}} = \frac{E_{mid}}{\Psi_{l\_pre} - \Psi_{l\_mid}}\frac{S_G}{S_{sap\_total}} \quad (6)$$

Although tree water capacitance is also known to affect changes in Ψ_l (Williams et al. 1998, Meinzer et al. 2009), we did not consider it here because the capacitance of *R. pseudoacacia* is modest in comparison with six other co-occurring species in North America (Jupa et al. 2016). Furthermore, although high tree water capacitance induces a time lag between the environmental conditions and sap flux at the base of the stem (Carrasco et al. 2015, Jupa et al. 2016), no time lag between J_s and D was observed in this study (data not shown) or in another study on *R. pseudoacacia* (Chen et al. 2014).

Model simulation of canopy-scale hydraulics and photosynthesis

Independently from the measured E, Ψ_{l_mid} and G_s, we computed canopy-scale gas exchange rates (A_c, E_c and G_s) and Ψ_l using the measured ecophysiological traits and meteorological data as model inputs (Figure 2). This model calculated G_s according to two criteria: the response of G_s to microenvironmental variables in the canopy and hydraulic safety (Williams et al. 1996).

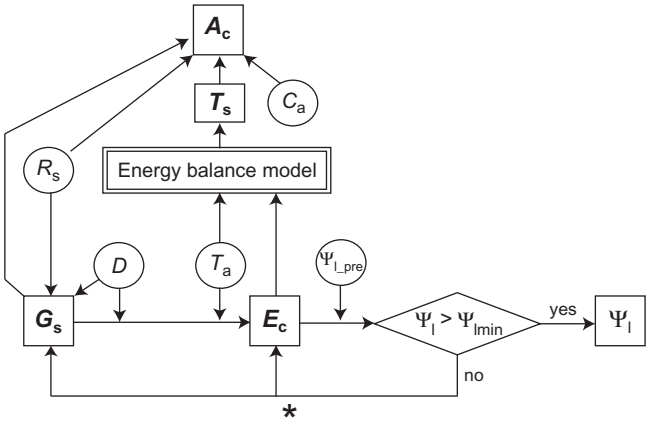

Figure 2. Diagram showing the effects of the various factors included in the calculations. Circles represent model inputs, which were measured in the field, and squares represent model outputs. Abbreviations: A_c, canopy-scale net photosynthetic rate; T_s, canopy surface temperature; C_a, atmospheric CO_2 concentration; R_s, shortwave solar radiation; D, vapor pressure deficit; T_a, air temperature; G_s, stomatal conductance; E_c, canopy-scale transpiration rate; Ψ_l, leaf water potential; Ψ_{l_pre}, predawn leaf water potential; Ψ_{lmin}, minimum leaf water potential. *In cases where the calculated Ψ_l was more negative than Ψ_{lmin}, E was recalculated to maintain Ψ_l at Ψ_{lmin} and this value was used for the further calculation of G_s and T_s.

To determine G_s as a function of various environmental variables, we calculated light-saturated G_s using the data we obtained for stomatal control (δ and G_{sref}) and D using Eq. (4). To account for variation in shortwave radiation (R_s, W m^{-2}), G_s was calculated as:

$$G_s = [G_{sref} - \delta\ln(D)]\frac{R_s}{R_s + \alpha} \quad (7)$$

where α was calculated by regressing G_s against R_s in each year (R Development Core Team 2006). The resulting G_s value was then used to calculate E_c according to Eq. (3). The leaf water potential Ψ_l was calculated using E_c, Ψ_{l_pre}, G_p and Eq. (6). Although Ψ_l varies even within a day and is thought to affect G_p, we do not take into consideration the responses in G_p to changes in Ψ_l at minute- or hour-scales but assumed a static G_p over a day (Williams et al. 1996).

When the calculated Ψ_l value was more negative than Ψ_{lmin}, we assumed that the trees had reduced G_s to maintain Ψ_l at Ψ_{lmin} (criterion of stomatal control for hydraulic safety). Equation (6) was used to calculate E_c with the input $\Psi_l = \Psi_{lmin}$ and this was then used to calculate G_s using Eq. (3). The recalculated E_c and G_s values were used for subsequent calculations.

E_c was used to calculate the surface temperature of the forest canopy (T_s, °C) using an energy balance model with the Penman–Monteith equation (Campbell and Norman 1998). The calculated G_s and T_s values were used to calculate A_c as a function of the measured environmental variables [atmospheric CO_2

concentration (C_a) and R_s] using a big leaf model (de Pury and Farquhar 1997).

Computed A, E_c, G_s and Ψ_l were used as surrogates for gas exchange and Ψ_l of *R. pseudoacacia* at the study site, and were computed by inputting the measured data (hereafter referred to as the 'control-base'). Where the input parameters varied with time (G_{sref}, δ, G_p and Ψ_{lmin}), only those that were measured in the same period were input.

Model simulation of gas exchange using different assumptions for tree hydraulics

In addition to the computation of canopy-scale gas exchange and hydraulics as a function of the measured data in each month (the control-case), model simulations were also run for cases with different assumptions for each of these inputs (Table 3). The three simulations (isohydric trees) were performed on the assumption that Ψ_{lmin} was maintained after it reached the annual least negative value in spring (Ψ_{lmin0}). In 2012, no values were obtained in spring and so G_p and Ψ_{lmin} were assumed to be the same as in spring 2013. Simulation of isohydric trees was run using $\Psi_{lmin} = \Psi_{lmin0}$ and all other parameters identical to the control-case, whereas simulation of isohydric constant-G_p trees used Ψ_{lmin0} as well as G_p at its highest annual value (G_{pmax}), and simulation of isohydric constant-G_p·G_{sref} trees used Ψ_{lmin0} and G_{pmax}, as well as δ and G_{sref} at their highest annual values (δ_{max} and $G_{srefmax}$).

Because isohydric trees had Ψ_{lmin0} as the input, it was expected to have a less negative Ψ_l than the control-case and to have lower gas exchange rates to prevent Ψ_l from becoming more negative than Ψ_{lmin0} [Eqs (3) and (6)]. By contrast, since the case of isohydric constant-G_p trees included G_{pmax}, which is thought to retain Ψ_l at a less negative value, it was expected to have higher gas exchange rates than isohydric trees [Eq. (6)]. Finally, the case of isohydric constant-G_p·G_{sref} trees, which included $G_{srefmax}$, was expected to have higher gas exchange rates than the cases of isohydric constant-G_p trees but a more negative Ψ_l.

The gas exchange rates and Ψ_l were also compared between the control-case and two simulation (anisohydric trees) in which a variable Ψ_{lmin} value was assumed. Anisohydric constant-G_p trees maintained G_p at G_{pmax} and so were expected to have a less negative Ψ_l than the control-case [Eq. (6)]. By contrast, anisohydric constant-G_p·G_{sref} trees included G_{pmax}, $G_{srefmax}$ and δ_{max}, and so were expected to have higher gas exchange rates and a more negative Ψ_l than anisohydric constant-G_p trees [Eq. (6)].

Results

Transpiration and its response to environmental variables

There was a clear seasonality in E, which was characterized by a peak in May–June followed by a gradual decrease and then a rapid decrease in mid–late September (Figure 1e). This seasonal trend did not vary among years, aside from a pronounced reduction in E in October 2013 and a high value in early August 2014. Although D reached a peak in July–August and remained high until September (Figure 1b), E slowly decreased after June in 2013 and July in 2012 due to a reduction in G_s (Figure 3a).

The G_s decreased in summer due to the high level of D and a reduction in G_{sref} (Figure 3b). G_{sref} reached the highest annual levels ($G_{srefmax}$) in May and then decreased in July in 2012 and 2013. However, in 2014, when there were fewer days with high D in early summer and many rainy days (Figure 1b and c), G_{sref} remained at $G_{srefmax}$ until July. On day of the year (DOY) 197 (2012), 181 (2013) and 213 (2014) and thereafter, the measured G_s under high R_s (>500 W m^{-2}) was consistently overestimated by the modeled G_s using Eq. (4) and G_{sref} for the month of July. We therefore assumed that G_{sref} experienced a sharp decrease on these dates in the subsequent analysis. Similarly, we assumed that there was a sharp decrease in G_{sref} on DOY 274 (2013) based on the comparison between the

Table 3. Description of the model simulations in which the gas exchange parameters δ (stomatal sensitivity to air pressure deficit) and G_{sref} (stomatal conductance per unit leaf area at an air pressure deficit of 1 kPa), and the plant hydraulic parameters Ψ_{lmin} (minimum leaf water potential) and G_p (plant hydraulic conductance) were changed based on the measured values.

	Ψ_{lmin}	δ, G_{sref}	G_p
Control–case	Measured[1]	Measured	Measured
Cases for isohydric trees			
1. Isohydric tree	Ψ_{lmin0}[2]	Measured	Measured
2. Isohydric constant-G_p tree	Ψ_{lmin0}	Measured	G_{pmax}[4]
3. Isohydric constant-G_p·G_{sref} tree	Ψ_{lmin0}	$G_{srefmax}$, δ_{max}[3]	G_{pmax}
Cases for anisohydric trees			
1. Anisohydric constant-G_p tree	Measured	Measured	G_{pmax}
2. Anisohydric constant-G_p·G_{sref} tree	Measured	$G_{srefmax}$, δ_{max}	G_{pmax}

[1]'Measured' indicates that the model used the value obtained during the same period as the calculation period.
[2]Annual least negative Ψ_{lmin} measured in spring (May–June).
[3]Annual maximum G_{sref} and δ at the time when $G_{sref} = G_{srefmax}$.
[4]Annual maximum G_p.

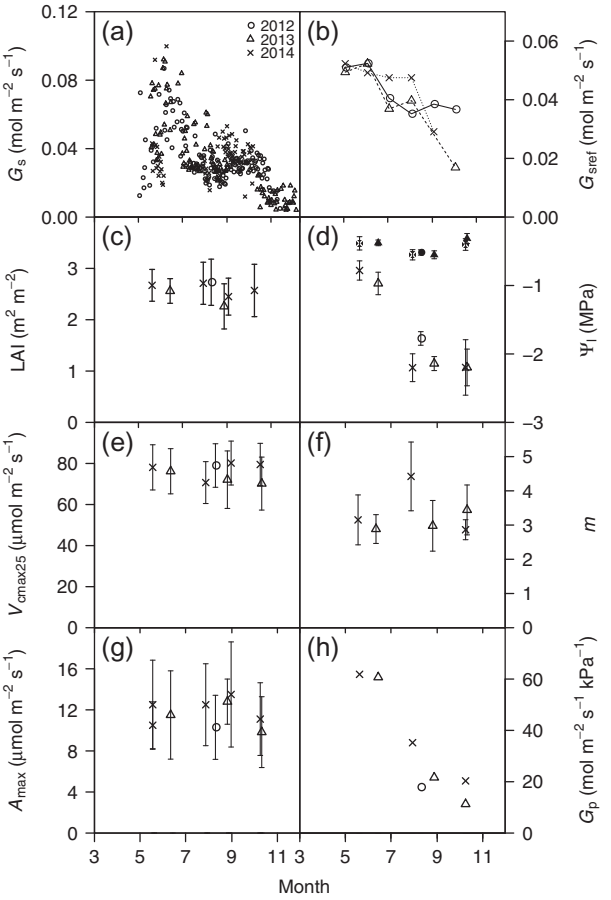

Figure 3. Seasonal trends in (a) stomatal conductance (G_s), (b) reference stomatal conductance (G_{sref}), (c) the leaf area index (LAI), (d) leaf water potential (Ψ_l), (e) the maximum rate of ribulose-1,5-bisphosphate (RuBP) carboxylation at 25 °C (V_{cmax25}), (f) stomatal sensitivity to environmental conditions (m), (g) light-saturated rate of net photosynthesis (A_{max}) and (h) plant hydraulic conductance for liquid water transport (G_p). Vertical bars represent standard deviations. In (d), the upper and lower points on each date represent the predawn and midday Ψ_l, respectively.

measured G_{sref} and modeled values using Eq. (4). There were no clear seasonal changes in LAI (Figure 3c).

The predawn Ψ_l (Ψ_{l_pre}) did not exhibit any clear seasonality and remained at ca −0.4 MPa throughout each year (Figure 3d). The midday Ψ_l (Ψ_{l_mid}) had the least negative annual values (Ψ_{lmin0}) in May–June and became more negative in early summer in each year. During the intensive measurements in spring, summer and autumn 2014, Ψ_l remained stable in the daytime when the leaves were exposed to direct solar radiation (data not shown) despite D exhibiting diurnal changes. The midday Ψ_{stem} (Ψ_{stem_mid}) was similar to Ψ_{l_mid} in spring and also became more negative in summer (−1 to −1.3 MPa). However, the reduction in Ψ_{stem_mid} after spring was smaller than that of Ψ_{l_mid}, indicating that the latter mainly resulted from the increased gradient in water potential between the stem and the leaf (data not shown).

For ecophysiological parameters at a leaf level, neither V_{cmax25} nor the sensitivity of g_{sc} to environmental conditions (m)

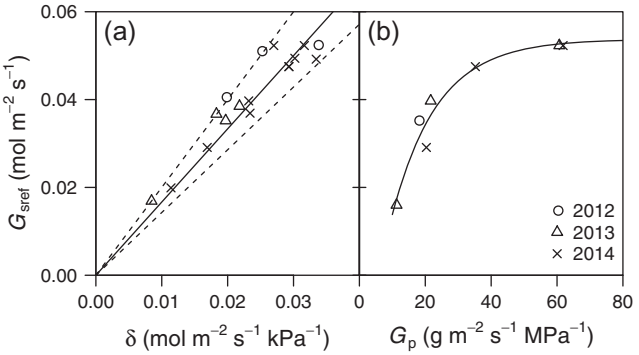

Figure 4. The relationship between stomatal conductance in the reference condition (G_{sref}) and (a) the slope of the stomatal conductance–ln (vapor pressure deficit) relationship (δ) and (b) plant hydraulic conductance for liquid water transport (G_p). An exponential equation was fit (solid curve) to the relationship.

changed from spring until 1 month before the beginning of leaf fall in November (Figure 3e and f). Leaves maintained a high V_{cmax25} even in the middle of summer when G_{sref} was low and the value of m remained low even in spring when D was low. Shaded leaves in the canopy exhibited lower levels of V_{cmax25} than crown surface leaves with no clear seasonality, suggesting that the profile of V_{cmax25} through the canopy remained consistent across seasons (data not shown).

Changes in G_{sref} were accompanied by changes in δ, with the ratio of δ to G_{sref} remaining at around 0.6 (Figure 4a). G_{sref} also increased with G_p along an asymptotic curve, suggesting that G_{sref} responded to changes in G_p when G_p fell below 20 g m^{-2} s^{-1} MPa^{-1} (Figure 4b), whereas changes in G_{sref} with G_p were negligible where G_p was >40 g m^{-2} s^{-1} MPa^{-1}. The degree of changes in G_p and G_{sref} was different and resulted in different Ψ_l before and after early summer (Figure 3d). The lowest G_p was observed in early October 2013. The relationship between G_{sref} and G_p allowed us to determine when G_p decreased based on the time course of G_{sref} (Figure 3b) in subsequent analyses, i.e., the timing of decreased G_{sref} was assumed to be the same as that of G_p.

Modeled canopy gas exchange rates

In the control-case, Ψ_l exhibited a sharp decrease on DOY 200 (2012), 180 (2013) and 213 (2014) (Figure 5a–c) due to a reduced G_p in association with G_{sref} (Figure 4b). Ψ_l remained low until the end of the growing season when D remained at the levels observed in spring. Although the cumulative E_c (E_{cum}) only modestly slowed the increase in Ψ_l after these time points (Figure 5j–l), trees experienced a clear decrease in daily A_c (A_{day}; Figure 5d–f) and a reduced rate of increase in cumulative A_c (A_{cum}, mol m^{-2}; Figure 5g–i). Decreased levels of G_{sref} and G_s lead to a reduction in A_c (Farquhar and Sharkey 1982) but did not cause a remarkable reduction in E_c, which was maintained at a level under high D after spring (Figure 1b). In 2013,

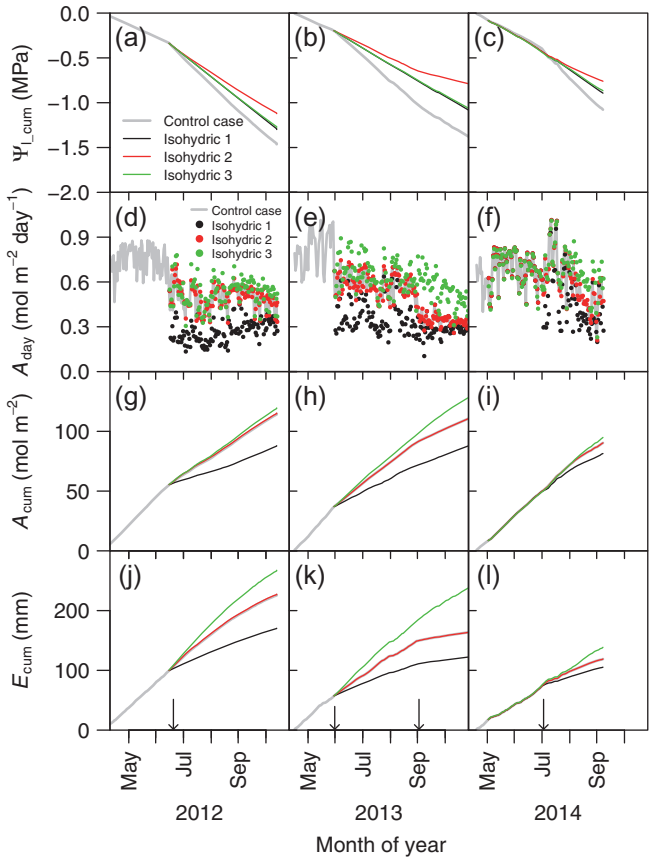

Figure 5. Seasonal trends in (a–c) the cumulative daily minimum leaf water potential (Ψ_l) normalized to the duration of monitoring in each year (Ψ_{l_cum}), (d–f) the simulated daily net photosynthetic rate at the canopy scale (A_{day}), (g–i) the cumulative A_c (A_{cum}) and (j–l) the cumulative canopy-scale transpiration rate (E_{cum}) in 2012, 2013 and 2014, respectively. Different colored lines and symbols represent different cases (control-case and the three cases for isohydric trees, respectively). Arrows represent day of year 200 (2012), 180, 274 (2013) and 213 (2014), respectively. For cases 1–3 of isohydric trees, refer to Table 3.

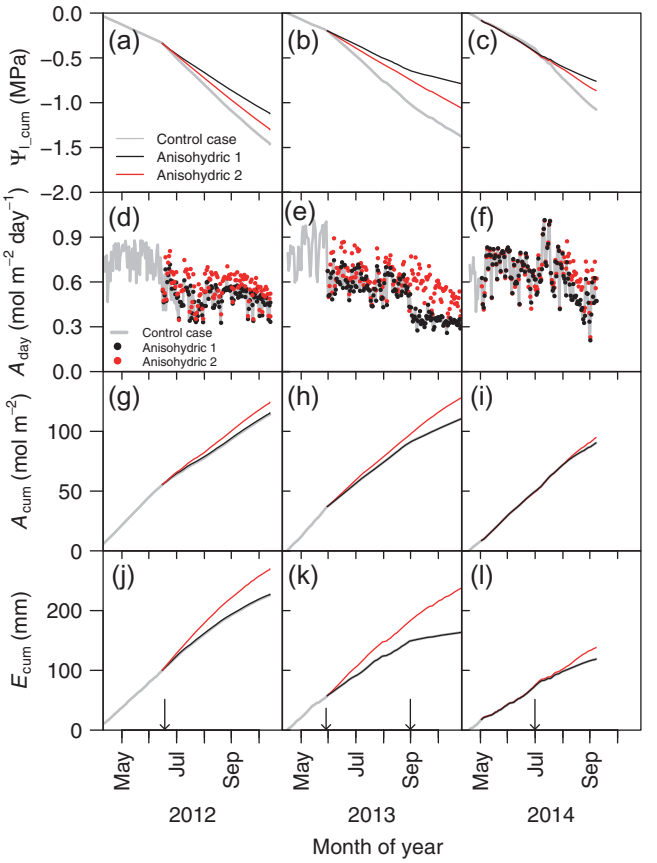

Figure 6. Seasonal trends in (a–c) the cumulative daily minimum leaf water potential (Ψ_l) normalized to the duration of monitoring in each year (Ψ_{l_cum}), (d–f) the simulated daily net photosynthetic rate at the canopy scale (A_{day}), (g–i) the cumulative A_c (A_{cum}) and (j–l) the cumulative canopy-scale transpiration rate (E_{cum}) in 2012, 2013 and 2014, respectively. Different colored lines and symbols represent different cases (control-case and the two cases for anisohydric trees, respectively). Arrows represent day of year 200 (2012), 180, 274 (2013) and 213 (2014), respectively. For cases 1 and 2 of anisohydric trees, refer to Table 3.

remarkable decreases in A_c and E_c were observed on DOY 274 when G_{sref} also exhibited a further decrease.

In isohydric trees, which maintained Ψ_l above Ψ_{lminO} (Table 3), Ψ_l was less negative than observed in the control-case in each year (Figure 5a–c). Furthermore, isohydric constant-G_p trees with $G_p = G_{pmax}$ exhibited an even less negative Ψ_l than isohydric trees. Although isohydric constant-G_p·G_{sref} trees also had $G_p = G_{pmax}$, Ψ_l was more negative than that of isohydric constant-G_p·G_{sref} trees and the same as in that of isohydric trees because of the higher G_{sref} (=$G_{srefmax}$) and E_c. In the c anisohydric constant-G_p trees with higher G_p (=G_{pmax}), Ψ_l was less negative than in the control-case (Figure 6a–c). In anisohydric constant-G_p·G_{sref} trees with G_{pmax} and $G_{srefmax}$, Ψ_l was more negative than in anisohydric constant-G_p·G_{sref} trees but less negative than in the control-case.

In isohydric trees, both A_c and E_c were lower than in the control-case in summer (Figure 5d–f and j–l) because E and G_s were reduced to maintain Ψ_l above Ψ_{lminO} (Figure 2). By contrast, isohydric constant-G_p trees achieved the same levels of A_c and E_c as the control-case by having $G_p = G_{pmax}$, while anisohydric constant-G_p·G_{sref} trees with G_{pmax} and $G_{srefmax}$ had not only a higher A_c than in the case-base but also a higher E_c. In anisohydric constant-G_p trees, A_c and E_c were as high as in the control-case despite the differences in G_p (Figure 6d–f and j–l), while in anisohydric constant-G_p·G_{sref} trees with $G_{srefmax}$, both A_c and E_c were higher than in the control-case.

Discussion

Leaf water potential and ecophysiological traits

In this study, we found that G_p and Ψ_{lmin} decreased in summer in *R. pseudoacacia*. However, this does not necessarily mean that *R. pseudoacacia* is a risk-taking species for cavitation. During the three monitoring years, *R. pseudoacacia* exhibited isohydric

stomatal control (Figure 4a; Oren et al. 1999) and maintained Ψ_{l_mid} at a constant level before summer and after summer, respectively (Figure 3d). These trees possessed a suite of ecophysiological traits that were effective for avoiding an increase in E and a decrease in Ψ_l, possibly reflecting acclimation to the evaporative summer on sandy soil with rapid drainage that occurs at this study site. The high G_{pmax} (Figure 4b) allowed *R. pseudoacacia* to achieve high levels of E without remarkably reducing Ψ_{l_mid} in spring (Figure 3d; Zhang and Cao 2009), which was less negative than the level observed in species growing in seasonal tropical forests during the rainy season that also experience drought in the subsequent dry season (Meinzer et al. 1999, Bucci et al. 2004, O'Grady et al. 2009), and similar to the level found in trees growing in a tropical rainforest (Rowland et al. 2015) and potted seedlings of *R. pseudoacacia* under sufficient watering (Yan et al. 2013).

Among the traits that affect E, LAI and m (or A/g_{sw}) were lower in the study trees (Figure 3c and f) than in *R. pseudoacacia* seedlings in potted experiments (Liu et al. 2013) or *R. pseudocacia* trees growing on the semiarid Loess Plateau (S. Du, Y. Miyazawa, N. Yamanaka, unpublished). Indeed, the observed m value was as low as that of tree species growing in the Mediterranean region (Martinez-Ferri et al. 2000), Australian savanna (Prior et al. 2004) and the monsoon region of Southeast Asia (Miyazawa et al. 2014) during the dry season. Yan et al. (2013) also showed that *R. pseudoacacia* started to reduce g_{sw} at a higher level of Ψ_l than other co-occurring species on the Loess Plateau under a progressive reduction in soil water availability. A low level of m even during the less evaporative spring appears to be less adaptive for increasing carbon gain (Farquhar and Sharkey 1982, Baldocchi et al. 2002). Since plants are known to express ecophysiological phenotypes that are suitable for survival in their native environments (Bourne et al. 2015), the closure of stomata under a high Ψ_{lminO} and the high G_{pmax} may reflect the water-abundant environments in this species' native region in North America, where trees do not need to risk opening their stomata during the less frequent droughts.

Although *R. pseudoacacia* exhibited a suite of species-specific ecophysiological traits that would be useful for avoiding excessive E under high evaporative demand, it did not exhibit a dynamic response in LAI, V_{cmax} or m (Figure 3c, e and f) to the decreased G_p during the evaporative summer. This contrasts with other species, which exhibit reduced levels of V_{cmax} (Xu and Baldocchi 2004), m (Baldocchi 1997, Miyazawa et al. 2014) and LAI (Wolfe et al. 2016) in response to drought, allowing them to balance the demand for E and water uptake from the soil (Katul et al. 2003). This lack of response to the sustained evaporative condition may be linked to this species' adaptation to the mesic environment in its native region [but see Rowland et al. (2015) for findings in trees subjected to a throughfall exclusion experiment in a tropical rainforest].

Robinia pseudoacacia decreased G_{sref} in summer in response to the reduced G_p (Figure 4b) to balance transpiration by leaves with the lowered water supply by the stem, as observed in other species (Meinzer et al. 1999, Addington et al. 2004, Anderegg et al. 2014). However, these changes in G_{sref} will only slightly contribute to hydraulic safety, i.e., maintenance of Ψ_l above Ψ_{lmin}, and the hydraulic safety required dynamic changes in Ψ_{lmin}. In isohydric constant-G_p trees, where Ψ_{lmin} was maintained at Ψ_{lminO}, the canopy experienced $\Psi_l = \Psi_{lmin}$ for a longer duration following a decrease in G_p in summer than in the other cases (Figure 5a–c), suggesting that the observed decrease in G_{sref} alone was not sufficient for hydraulic safety in summer (Martínez-Vilalta et al. 2014). In this study, the observed decrease in G_{sref} by 30% in response to a decrease in G_p was modest (Figure 4b) compared with conifer trees in a temperate forest, which reduce G_{sref} by 50% (Addington et al. 2004). Furthermore, trees growing in the Brazilian cerrado also exhibit more pronounced decreases in G_p and G_s in the dry season than were observed here (Meinzer et al. 1999).

The lowered Ψ_{lmin} in early summer did not induce a further progressive reduction in G_p or G_s, except for in October 2013 (Figure 4a and b), and also did not reduce A_c, suggesting that run-away cavitation was avoided (Tyree and Sperry 1988). This plastic change in Ψ_{lmin} without run-away cavitation contrasts with the findings of previous studies (Meinzer et al. 2009, Choat et al. 2012), which have shown that a number of species around the world have a small safety margin between the actual Ψ_{lmin} and the critical level for cavitation. The observed G_p in summer was less than 30% of G_{pmax}, and so Ψ_{lmin} in summer was below the level, which is used as the critical level for cavitation in many studies (Ψ_l at which G_p is 50% of the maximum) (Choat et al. 2012, Meinzer et al. 2009, but see Carrasco et al. 2015).

Plastic changes in Ψ_{lmin} allow high carbon gains with a reduced G_p

Robinia pseudoacacia trees offset the potentially strong effect of decreased G_p on photosynthesis by concomitantly decreasing Ψ_{lmin} (control-case, Figure 5), allowing A_c to remain as high as in the other cases. Previous studies have found a reduced G_p in focal trees (Meinzer et al. 1999, Addington et al. 2004, Domec et al. 2009, Anderegg et al. 2014) but have not reported a concomitant reduction in Ψ_{lmin} as a compensatory mechanism for mitigating the associated reduction in G_s. Therefore, it is interesting that this species, which has isohydric stomatal control (Oren et al. 1999; Figure 4a) and maintained Ψ_{l_mid} at Ψ_{lmin} within each season, regularly changed Ψ_{lmin} among seasons within each year (Figure 3d). Trees with low plant hydraulic conductance have been shown to have more negative midday Ψ_l levels in comparisons among species (Bucci et al. 2004) and within species (Bucci et al. 2006). In this study, *R. pseudoacacia* trees showed a similar dynamic control of Ψ_{lmin} within a year in response to the annual decrease in G_p (Figure 4b).

Model simulation revealed that *R. pseudoacacia* achieved as high an A_c in summer in the control-case as in the other cases that included alternative potential ecophysiological responses to changing environments due to its ability to plastically change Ψ_{lmin}. Despite the lowered G_p, the control-case prevented Ψ_l from becoming as negative as Ψ_{lmin} after summer and achieved G_s as expressed by Eq. (4) during most periods under high R_s, as seen in isohydric constant-G_p trees and anisohydric constant-G_p trees. By contrast, in isohydric trees, A_{cum} was ~9.9–23.2% lower than in the control-case due to the frequent reduction of G_s to maintain Ψ_l above Ψ_{lminO}. These findings demonstrate that as long as the lowered Ψ_{lmin} does not involve a progressive decrease in G_p (Figure 4b), decreasing Ψ_{lmin} is an effective strategy for increasing A_c in environments where G_p is forced to low levels by drought on an annual basis.

The maintenance of both G_p and G_{sref} at high levels (isohydric constant-G_p·G_{sref} trees and anisohydric constant-G_p·G_{sref} trees) not only allowed the trees to achieve a higher A_c than in the control-case but also increased E_c, which increases the risk of soil water depletion. The sand substrate and shallow root zone at this study site mean that increased water use beyond the level observed in this study (Figure 1e) may seriously reduce Ψ_{l_pre}, G_s and A_c in summer, as simulated for trees growing in tropical seasonal forests during the dry season (Tanaka et al. 2009). Thus, *R. pseudoacacia* may be balancing its water use and carbon gain by seasonally controlling G_{sref} to avoid excessive soil water depletion, and by maintaining relatively low levels of LAI and m (Figure 3c and f).

The plastic change in Ψ_{lmin} in response to a lowered G_p is related to the fact that G_p was not recovered until the following year (Figure 4b) and cavitation occurred in the leaf blades. Recent studies have found that cavitation is not an extreme event under severe water stress but rather can be recovered from (McCulloh and Meinzer 2015). Many species reduce G_p or other measures of plant hydraulic conductance for liquid water transport (Brodribb and Holbrook 2003, Addington et al. 2004, Domec et al. 2009, Anderegg et al. 2014). However, the absence of recovery of G_p in *R. pseudoacacia* means that this species has to photosynthesize at low levels of G_p and G_{sref} (Figure 4b) during the rest of the growing season, the length of which varies among years (Figure 3b). Furthermore, even if leaves do experience further cavitation, they can be replaced by new leaves the following spring, unlike roots or stems, which cannot be easily replaced. The veins in a leaf blade worked as a 'hydraulic fuse' that prevents cavitation in the more expensive woody portion of the water transport pathway (Bucci et al. 2012) by inducing a reduced G_s (Hubbard et al. 2001; Figure 4b) and maintaining Ψ_{stem} above the level for cavitation (Wang et al. 2014). Therefore, the low risk of sustained damage on the expensive hydraulic system in roots and stems may have driven *R. pseudoacacia* to plastically decrease Ψ_{lmin}.

Conclusion

In this study, we found that *R. pseudoacacia* alleviates the environmental impact of seasonal drought conditions on A_c by seasonally changing Ψ_{lmin}. The production of more negative levels of Ψ_{lmin} at the risk of further cavitation is an important response for maintaining A_c at high levels at this study site (Figures 5 and 6) and possibly also in other plantation areas, including the arid regions of the Loess Plateau in China. The maintenance of a high V_{cmax} throughout the year also contributes to maintaining a high A_c even at low levels of G_s and C_i (Figure 3e). However, although A_c is effectively promoted by changing Ψ_{lmin} as long as G_p is maintained at the levels seen during most periods in this study, reducing Ψ_{lmin} is a risky strategy: if leaves in the early stage of the growing season experience serious reductions in G_p and G_{sref} to the level that occurred in October 2013 (Figure 3b), they will likely photosynthesize at a negligible level throughout the rest of the growing season (Figure 5b and e). Thus, this risky strategy for changing Ψ_{lmin} may partly explain the serious dieback of this tree that has been widely observed in plantations in Japan and the Loess Plateau in China (Yamanaka et al. 2014).

Abbreviations

A (μmol m^{-2} s^{-1})	net photosynthetic rate
K_G (kPa m^3 kg^{-1})	nonversion function from transpiration rate to stomatal conductance
c (mol m^{-3})	molar air density
C_a (μmol mol^{-1})	air CO_2 concentration
C_s (μmol mol^{-1})	CO_2 concentration at leaf surface
C_i (μmol mol^{-1})	leaf intercellular CO_2 concentration
D (kPa)	air vapor pressure deficit
δ [mol m^{-2} s^{-1} ln (kPa)$^{-1}$]	stomatal sensitivity to D
DBH (cm)	diameter at breast height
ΔT (°C)	difference in temperature between two probes of a sap flux sensor
ΔT_{max} (°C)	ΔT at sap flux = 0.
$\Delta\Psi_l$ (MPa)	difference in leaf water potential between predawn and midday
E (g m^{-2} s^{-1} or mm day^{-1})	transpiration rate (leaf- or stand-level)
F_d (g m^{-2} s^{-1})	sap flux
G_p (g m^{-2} s^{-1} MPa^{-1})	plant hydraulic conductivity
G_s (mol m^{-2} s^{-1})	stomatal conductance per unit leaf area measured using sap flux data
g_{sw} (mol m^{-2} s^{-1})	leaf-level stomatal conductance measured using leaf-level data
G_{sref} (mol m^{-2} s^{-1})	G_s at D = 1 kPa
h_r	relative humidity at leaf surface

J_s (g m^{-2} s^{-1})	sap flux of the stand
m	stomatal sensitivity to environmental and leaf ecophysiological variables
θ_{soil}	volumetric soil water content
R_d (μmol m^{-2} s^{-1})	dark respiration rate
R_s (W m^{-2})	shortwave radiation
S_s (m^2)	sapwood area
S_G (m^2)	ground area of a plot
T_a (°C)	air temperature
T_l (°C)	leaf temperature
V_{cmax25} (μmol m^{-2} s^{-1})	RuBP carboxylation rate standardized at a leaf temperature of 25 °C
Ψ_l (MPa)	leaf water potential
Ψ_{lmin} (MPa)	minimum leaf water potential
Ψ_{lminO} (MPa)	annual least negative value of minimum leaf water potential
Ψ_{stem} (MPa)	stem water potential (subscripts)
c	values at canopy-scale
cum	cumulative value since the beginning of calculation
day	value per day
max	annual maximum value
mid	value obtained at midday
pre	value obtained predawn

Acknowledgments

We thank the staffs of Aridland Research Center, Tottori University for the supports of the monitoring of sap flux and meteorological variables. We thank Drs Makiko Tateishi and Fumiko Iwanaga for the supports of field measurements. The authors would like to thank Enago (www.enago.jp) for the English language review.

Conflict of interest

None declared.

Funding

This study was financially supported by the Japan Society for the Promotion of Science (JSPS) for Grant-in-Aid for Encouragement of Scientists, a Grant-in-Aid for Scientific Research, and the National Natural Science Foundation of China–JSPS bilateral joint research project (Nos. 41471440 and 41411140035). This study was also partly funded by the Joint Research Program of Arid Land Research Center, Tottori University (No. h25-62).

References

Adams HD, Guardiola-Claramonte M, Barron-Gafford GA, Villegas JC, Breshears DD, Zou CB, Troch PA, Huxman TE (2009) Temperature sensitivity of drought-induced tree mortality portends increased regional die-off under global-change-type drought. Proc Natl Acad Sci USA 106:7063–7066.

Addington RN, Mitchell RJ, Oren R, Donovan LA (2004) Stomatal sensitivity to vapor pressure deficit and its relationship to hydraulic conductance in *Pinus palustris*. Tree Physiol 24:561–569.

Anderegg WRL, Anderegg LDL, Berry JA, Field CB (2014) Loss of whole-tree hydraulic conductance during severe drought and multi-year forest die-off. Oecologia 175:11–23.

Baldocchi D (1997) Measuring and modelling carbon dioxide and water vapour exchange over a temperate broad-leaved forest during the 1995 summer drought. Plant Cell Environ 20:1108–1122.

Baldocchi DD, Wilson KB, Gu LH (2002) How the environment, canopy structure and canopy physiological functioning influence carbon, water and energy fluxes of a temperate broad-leaved deciduous forest-an assessment with the biophysical model CANOAK. Tree Physiol 22: 1065–1077.

Ball JT, Woodrow IE, Berry JA (1987) A model predicting stomatal conductance and its contribution to the control of photosynthesis under different environmental conditions. In: Biggins J (ed) Progress in photosynthesis research. Martinus-Nijhoff Publishers, Dordrecht, The Netherlands, pp 221–224.

Binks O, Meir P, Rowland L et al. (2016) Plasticity in leaf-level water relations of tropical rainforest trees in response to experimental drought. New Phytol 211:477–488.

Bourne AE, Haigh AM, Ellsworth DS (2015) Stomatal sensitivity to vapour pressure deficit relates to climate of origin in Eucalyptus species. Tree Physiol 35:266–278.

Brodribb TJ, Holbrook NM (2003) Changes in leaf hydraulic conductance during leaf shedding in seasonally dry tropical forest. New Phytol 158: 295–303.

Bucci SJ, Goldstein G, Meinzer FC, Scholz FG, Franco AC, Bustamante M (2004) Functional convergence in hydraulic architecture and water relations of tropical savanna trees: from leaf to whole plant. Tree Physiol 24:891–899.

Bucci SJ, Scholz FG, Goldstein G, Meinzer FC, Franco AC, Campanello PI, Villalobos-Vega R, Bustamante M, Miralles-Wilhelm F (2006) Nutrient availability constrains the hydraulic architecture and water relations of savannah trees. Plant Cell Environ 29:2153–2167.

Bucci SJ, Scholz FG, Campanello PI et al. (2012) Hydraulic differences along the water transport system of South American Nothofagus species: do leaves protect the stem functionality? Tree Physiol 32:880–893.

Campbell GS, Norman JM (1998) An introduction to environmental biophysics, 2nd edn. Springer, New York, NY.

Carrasco LO, Bucci SJ, Di Francescantonio D et al. (2015) Water storage dynamics in the main stem of subtropical tree species differing in wood density, growth rate and life history traits. Tree Physiol 35: 354–365.

Chen LX, Zhang ZQ, Zeppel M, Liu CF, Guo JT, Zhu JZ, Zhang XP, Zhang JJ, Zha TG (2014) Response of transpiration to rain pulses for two tree species in a semiarid plantation. Int J Biometeorol 58:1569–1581.

Choat B, Jansen S, Brodribb TJ et al. (2012) Global convergence in the vulnerability of forests to drought. Nature 491:752–755.

Clearwater MJ, Meinzer FC, Andrade JL, Goldstein G, Holbrook NM (1999) Potential errors in measurement of nonuniform sap flow using heat dissipation probes. Tree Physiol 19:681–687.

de Pury DGG, Farquhar GD (1997) Simple scaling of photosynthesis from leaves to canopies without the errors of big-leaf models. Plant Cell Environ 20:537–557.

Domec JC, Noormets A, King JS, Sun G, McNulty SG, Gavazzi MJ, Boggs JL, Treasure EA (2009) Decoupling the influence of leaf and root hydraulic conductances on stomatal conductance and its sensitivity to vapour pressure deficit as soil dries in a drained loblolly pine plantation. Plant Cell Environ 32:980–991.

Du S, Wang YL, Kume T, Zhang JG, Otsuki K, Yamanaka N, Liu GB (2011) Sapflow characteristics and climatic responses in three forest species in the semiarid Loess Plateau region of China. Agric For Meteorol 151: 1–10.

Farquhar GD, Sharkey TD (1982) Stomatal conductance and photosynthesis. Annu Rev Plant Physiol Plant Molec Biol 33:317–345.

Farquhar GD, Caemmerer SV, Berry JA (1980) A biochemical-model of photosynthetic CO_2 assimilation in leaves of C-3 species. Planta 149: 78–90.

Granier A (1987) Evaluation of transpiration in a douglas-fir stand by means of sap flow measurements. Tree Physiol 3:309–319.

Hacke UG, Sperry JS, Ewers BE, Ellsworth DS, Schafer KVR, Oren R (2000) Influence of soil porosity on water use in *Pinus taeda*. Oecologia 124:495–505.

Harley PC, Thomas RB, Reynolds JF, Strain BR (1992) Modeling photosynthesis of cotton grown in elevated CO_2. Plant Cell Environ 15: 271–282.

Hubbard RM, Ryan MG, Stiller V, Sperry JS (2001) Stomatal conductance and photosynthesis vary linearly with plant hydraulic conductance in ponderosa pine. Plant Cell Environ 24:113–121.

James SA, Clearwater MJ, Meinzer FC, Goldstein G (2002) Heat dissipation sensors of variable length for the measurement of sap flow in trees with deep sapwood. Tree Physiol 22:277–283.

Jones HG, Sutherland RA (1991) Stomatal control of xylem embolism. Plant Cell Environ 14:607–612.

Jupa R, Plavcová L, Gloser V, Jansen S (2016) Linking xylem water storage with anatomical parameters in five temperate tree species. Tree Physiol 212:383–395.

Katul G, Leuning R, Oren R (2003) Relationship between plant hydraulic and biochemical properties derived from a steady-state coupled water and carbon transport model. Plant Cell Environ 26:339–350.

Kimura K, Yamasaki S (2003) Accurate root length and diameter measurement using NIH Image: use of Pythagorean distance for diameter estimation. Plant Soil 254:305–315.

Kondo J, Xu JC (1997) Seasonal variations in the heat and water balances for nonvegetated surfaces. J Appl Meteor 36:1676–1695.

Kumagai T, Porporato A (2012) Strategies of a Bornean tropical rainforest water use as a function of rainfall regime: isohydric or anisohydric? Plant Cell Environ 35:61–71.

Kumagai T, Aoki S, Shimizu T, Otsuki K (2007) Sap flow estimates of stand transpiration at two slope positions in a Japanese cedar forest watershed. Tree Physiol 27:161–168.

Liu XP, Fan YY, Long JX, Wei RF, Kjelgren R, Gong CM, Zhao J (2013) Effects of soil water and nitrogen availability on photosynthesis and water use efficiency of *Robinia pseudoacacia* seedlings. J Environ Sci (China) 25:585–595.

Manzoni S, Vico G, Katul G, Palmroth S, Jackson RB, Porporato A (2013) Hydraulic limits on maximum plant transpiration and the emergence of the safety-efficiency trade-off. New Phytol 198:169–178.

Martinez-Ferri E, Balaguer L, Valladares F, Chico JM, Manrique E (2000) Energy dissipation in drought-avoiding and drought-tolerant tree species at midday during the Mediterranean summer. Tree Physiol 20: 131–138.

Martínez-Vilalta J, Poyatos R, Aguadé D, Retana J, Mencuccini M (2014) A new look at water transport regulation in plants. New Phytol 204: 105–115.

McCulloh KA, Meinzer FC (2015) Further evidence that some plants can lose and regain hydraulic function daily. Tree Physiol 35:691–693.

Meinzer FC, Goldstein G, Franco AC, Bustamante M, Igler E, Jackson P, Caldas L, Rundel PW (1999) Atmospheric and hydraulic limitations on transpiration in Brazilian cerrado woody species. Funct Ecol 13:273–282.

Meinzer FC, Johnson DM, Lachenbruch B, McCulloh KA, Woodruff DR (2009) Xylem hydraulic safety margins in woody plants: coordination of stomatal control of xylem tension with hydraulic capacitance. Funct Ecol 23:922–930.

Miyazawa Y, Tateishi M, Komatsu H, Iwanaga F, Mizoue N, Ma V, Sokh H, Kumagai T (2014) Implications of leaf-scale physiology for the tree transpiration characteristics under seasonal flooding and drought in central Cambodia. Agric For Meteorol 198–199:221–231.

Naithani KJ, Ewers BE, Pendall E (2012) Sap flux-scaled transpiration and stomatal conductance response to soil and atmospheric drought in a semi-arid sagebrush ecosystem. J Hydrol 464:176–185.

O'Grady AP, Cook PG, Eamus D, Duguid A, Wischusen JDH, Fass T, Worldege D (2009) Convergence of tree water use within an arid-zone woodland. Oecologia 160:643–655.

Oishi AC, Oren R, Stoy PC (2008) Estimating components of forest evapotranspiration: a footprint approach for scaling sap flux measurements. Agric For Meteorol 148:1719–1732.

Oren R, Sperry JS, Katul GG, Pataki DE, Ewers BE, Phillips N, Schafer KVR (1999) Survey and synthesis of intra- and interspecific variation in stomatal sensitivity to vapour pressure deficit. Plant Cell Environ 22:1515–1526.

Phillips N, Oren R (1998) A comparison of daily representations of canopy conductance based on two conditional time-averaging methods and the dependence of daily conductance on environmental factors. Ann Sci For 55:217–235.

Prior LD, Bowman D, Eamus D (2004) Seasonal differences in leaf attributes in Australian tropical tree species: family and habitat comparisons. Funct Ecol 18:707–718.

R Development Core Team (2006) R: A language and environment for statistical computing. R Foundation for Statistical Computing, Vienna, Austria.

Rowland L, da Costa ACL, Galbraith DR et al. (2015) Death from drought in tropical forests is triggered by hydraulics not carbon starvation. Nature 528:119–122.

Saliendra NZ, Sperry JS, Comstock JP (1995) Influence of leaf water status on stomatal response to humidity, hydraulic conductance, and soil drought in *Betula occidentalis*. Planta 196:357–366.

Sokal RR, Rohlf FJ (1995) Biometry, 3rd edn. Freeman, New York, NY.

Tanaka-Oda A, Kenzo T, Koretsune S, Sasaki H, Fukuda K (2010) Ontogenetic changes in water-use efficiency (delta C-13) and leaf traits differ among tree species growing in a semiarid region of the Loess Plateau, China. For Ecol Manage 259:953–957.

Tanaka K, Yoshifuji N, Tanaka N, Shiraki K, Tantasirin C, Suzuki M (2009) Water budget and the consequent duration of canopy carbon gain in a teak plantation in a dry tropical region: analysis using a soil–plant–air continuum multilayer model. Ecol Model 220:1534–1543.

Tyree MT, Sperry JS (1988) Do woody-plants operate near the point of catastrophic xylem dysfunction caused by dynamic water-stress – answers from a model. Plant Physiol 88:574–580.

von Caemmerer S, Evans JR, Hudson GS, Andrews TJ (1994) The kinetics of ribulose-1,5-bisphosphate carboxylase/oxygenase in-vivo inferred from measurements of photosynthesis in leaves of transgenic Tobacco. Planta 195:88–97.

Wang RQ, Zhang LL, Zhang SX, Cai J, Tyree MT (2014) Water relations of *Robinia pseudoacacia* L.: do vessels cavitate and refill diurnally or are R-shaped curves invalid in *Robinia*? Plant Cell Environ 37:2667–2678.

Williams M, Rastetter EB, Fernandes DN et al. (1996) Modelling the soil-plant-atmosphere continuum in a *Quercus-Acer* stand at Harvard forest: the regulation of stomatal conductance by light, nitrogen and soil/plant hydraulic properties. Plant Cell Environ 19:911–927.

Williams M, Malhi Y, Nobre AD, Rastetter EB, Grace J, Pereira MGP (1998) Seasonal variation in net carbon exchange and evapotranspiration in a Brazilian rain forest: a modelling analysis. Plant Cell Environ 21: 953–968.

Wolfe BT, Sperry JS, Kursar TA (2016) Does leaf shedding protect stems from cavitation during seasonal droughts? A test of the hydraulic fuse hypothesis. New Phytol 212:1007–1018.

Xu LK, Baldocchi DD (2004) Seasonal variation in carbon dioxide exchange over a Mediterranean annual grassland in California. Agric For Meteorol 123:79–96.

Yamanaka N, Hou QC, Du S (2014) Vegetation of the Loess Plateau. In: Tsunekawa A, Liu G, Yamanaka N, Du S (eds) Restoration and development of the degraded Loess Plateau, China. Springer, Tokyo, pp 49–60.

Yan MJ, Yamamoto M, Yamanaka N, Yamamoto F, Liu GB, Du S (2013) A comparison of pressure-volume curves with and without rehydration pretreatment in eight woody species of the semiarid Loess Plateau. Acta Physiol Plant 35:1051–1060.

Zhang JL, Cao KF (2009) Stem hydraulics mediates leaf water status, carbon gain, nutrient use efficiencies and plant growth rates across dipterocarp species. Funct Ecol 23:658–667.

Zheng F, Wang B (2014) Soil erosion in the Loess Plateau region of China. In: Tsunekawa A, Liu G, Yamanaka N, Du S (eds) Restoration and development of the degraded Loess Plateau, China. Springer, Tokyo, pp 77–92.